SUPPLEMENTARY TABLES AND LEGENDS:

Supplemental Figure 1:

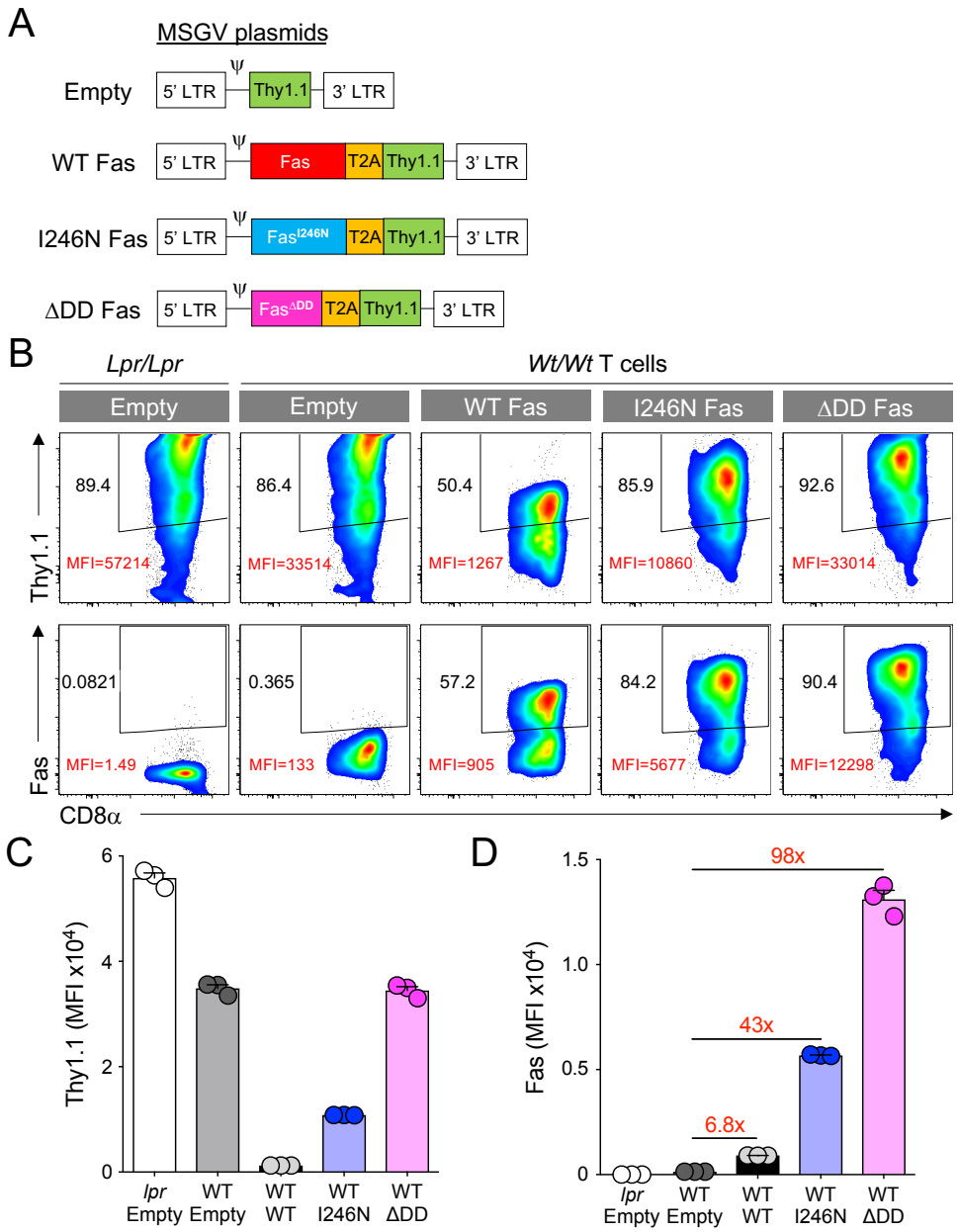

Supplemental Figure 1: Design and expression of retrovirally-encoded Fas DNR constructs and controls in mouse CD8⁺ T cells. (A) Schematic overview of the designs for retroviral constructs encoding murine wildtype (WT) Fas or mutant versions of Fas impaired in their ability to bind the intracellular adapter molecule Fas-associated via death domain. WT Fas, Fas^{I246N}, or $Fas^{\Delta DD}$ were cloned into an MSGV1 expression vector in front of a T2A cleavage site and the Thy1.1 reporter gene. An empty vector containing only the Thy1.1 reporter gene (Empty) was used as a negative control. **(B)** Representative FACS plots and summary bar graphs of **(C)** Thy1.1 and **(D)** Fas expression 4d following retroviral transduction of Fas-deficient B6-lpr or WT CD8α⁺ T cells. The percentage of gated Thy1.1⁺ or Fas⁺ cells is shown in black, MFI of Thy1.1⁺ or Fas⁺ cells is shown in red **(C)**. Fold change in Fas MFI over endogenous, WT Fas expression in WT, Empty-transduced cells is shown in red in **(D)**. Data in (**C**) and (**D**) are displayed as mean ± SEM with *n*=3 per condition and is representative of 12 independent experiments.

Supplemental Figure 2:

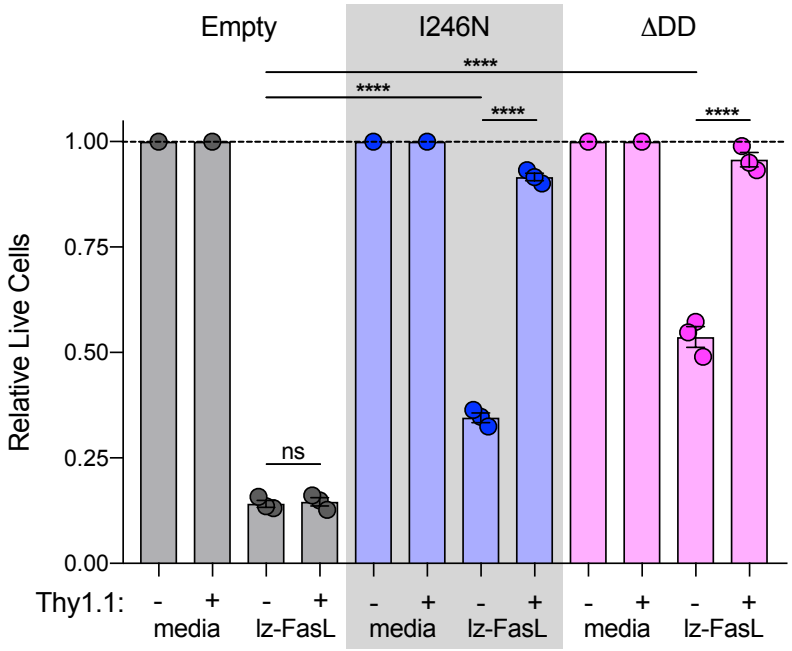

Supplemental Figure 2: Fas DNRs can protect non-transduced cells from FasL-mediated apoptosis. Summary bar graph showing the relative frequency of cell viability of non-transduced and transduced T cells after 20h following exposure to lz-FasL (100 ng mL^{-1}). Results shown after gating on live $CD8\alpha^{+}$ lymphocytes, and viability shown relative to the media for each transduction condition. Data shown is representative of 3 independently performed experiments and is displayed as mean ± SEM with $n = 3$ per condition. ****$P<0.0001$, ns = not significant (one-way ANOVA, corrected with Tukey's multiple comparisons).

Supplemental Figure 3:

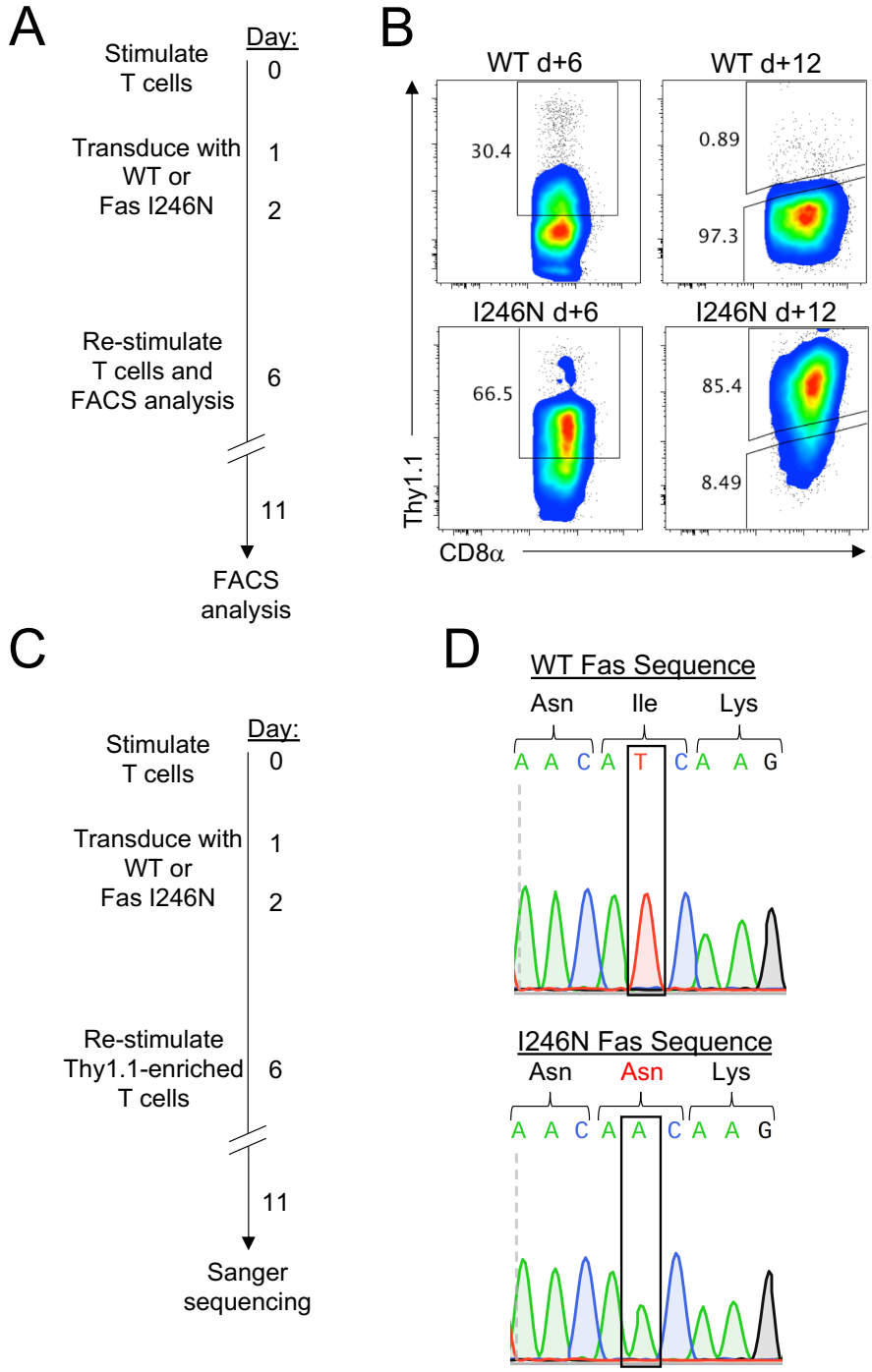

Supplemental Figure 3: Expression of FasI246N in T cells does not cause reversion to WT Fas. (A) Experimental timeline for the stimulation, retroviral transduction, and analysis of WT CD8α$^+$ T cells modified with Fas^{WT} or Fas^{I246N}. **(B)** Representative FACS plots of Thy1.1 expression at days 6 and 12 for Fas^{WT} or Fas^{I246N} transduced cells. **(C)** Experimental timeline for the stimulation, transduction, Thy1.1-enrichment, and sequencing of WT CD8α$^+$ T cells modified with Fas^{WT} or Fas^{I246N}. **(D)** Representative sequencing data showing WT Fas maintains the A-T-C sequence encoding the isoleucine at amino acid position 246, whereas the Fas^{I246N} sequence is A-A-C, encoding an asparagine at amino acid position 246 in the introduced Fas DNR construct.

Supplemental Figure 4:

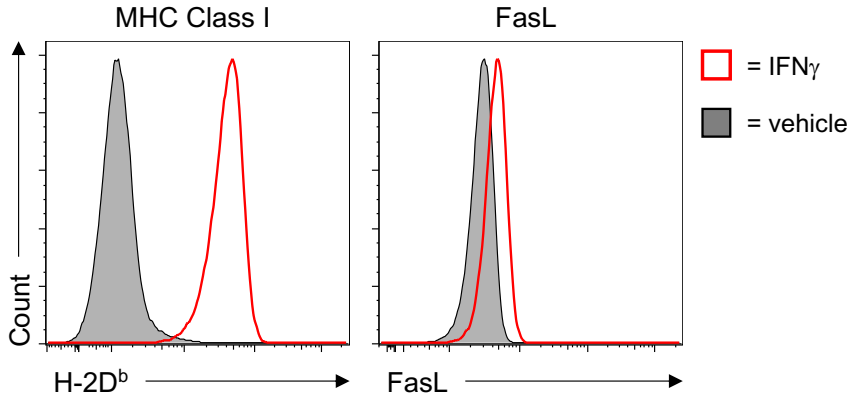

Supplemental Figure 4: IFNγ upregulates FasL on surface of B16 tumor cells. B16 cells were treated with vehicle (PBS) or IFNγ (100 ng mL^{-1}) for 24 hours, then analyzed for surface expression of MHC Class I (H-2D^b; left panel) or FasL (right panel) by flow cytometry.

Supplemental Figure 5:

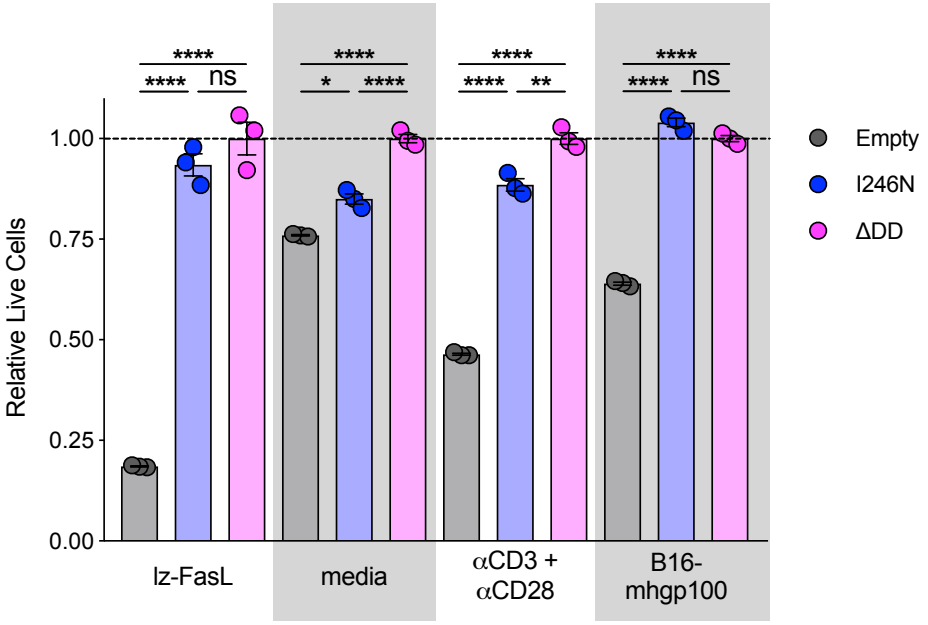

Supplemental Figure 5: T cells engineered with Fas DNRs prevent apoptosis from various stimuli. Summary bar graph showing the relative frequency of cell viability of transduced T cells after 20h following exposure to lz-FasL (100 ng mL^{-1}). Results are shown after gating on $Thy1.1^{+}$ cells, and viability is shown relative to $Fas^{\Delta DD}$. Data shown is representative of 10 independently performed experiments and is displayed as mean ± SEM with $n = 3$ per condition. *P<0.05 **P<0.01 ****P<0.0001, ns = not significant (one-way ANOVA, corrected with Tukey's multiple comparisons).

Supplemental Figure 6:

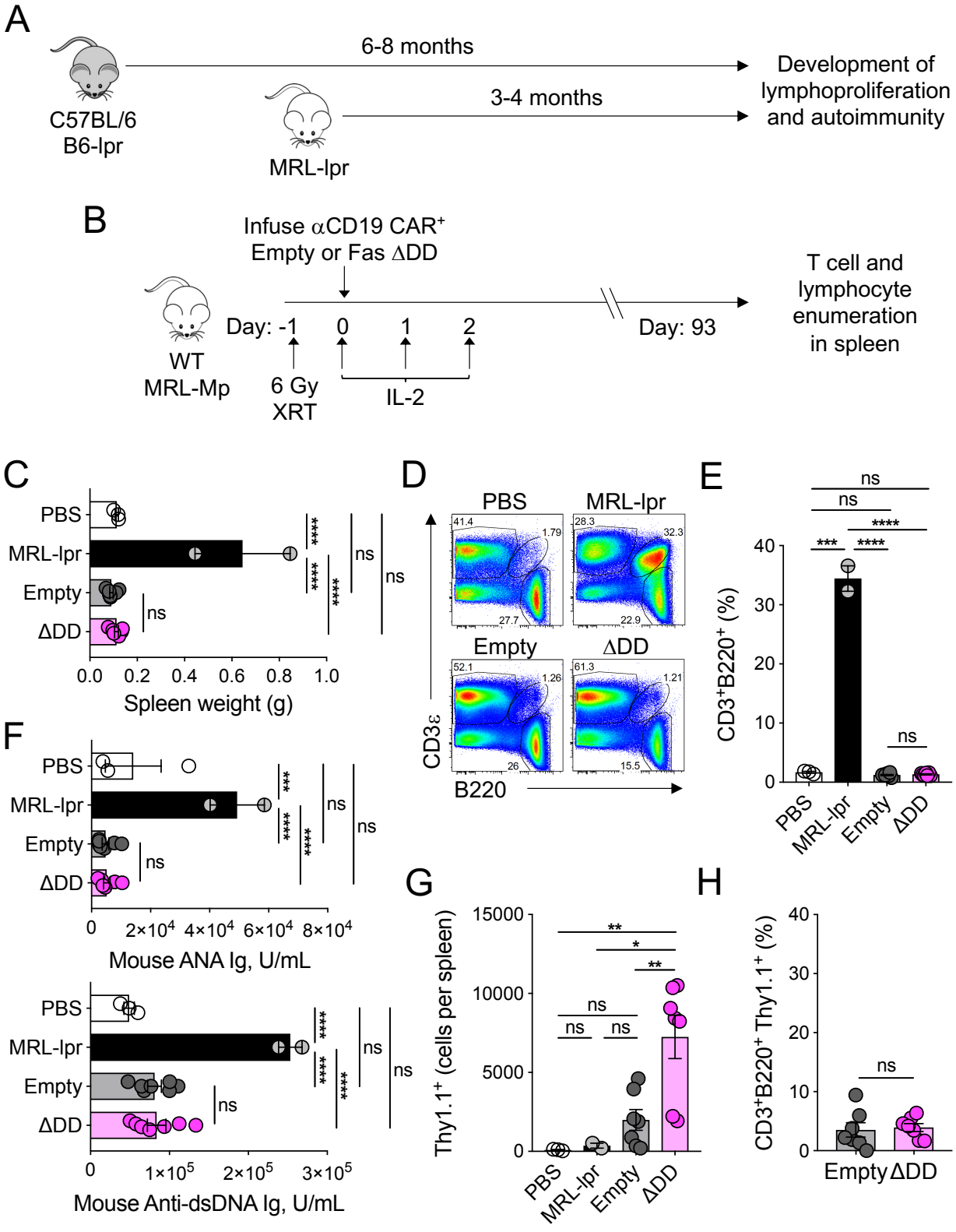

Supplemental Figure 6. Fas DNR expression does not induce lymphoproliferation in the ALPS-susceptible MRL strain. (A) Schematic comparing the onset of lymphoproliferation in C57BL/6 B6-lpr mice at 6-9 months (top) to the MRL-lpr strain at 3-4 months. **(B)** Experimental design to analyze long-term persistence of WT anti-CD19 CAR expressing CD8α^+ T cells modified with $Fas^{\Delta DD}$ or empty vector control in WT MRL-Mp mice. A total of $3x10^6$ of anti-CD19 CAR^+ CD8α^+ T cells were infused i.v. into sublethally irradiated (6 Gy XRT) mice. Recipient mice received IL-2 by daily i.p. injection for 3d and the spleens were harvested for analysis after 93d. (**C**) Summary numbers of spleen weight in recipient mice, compared to age-matched wild type mice and Fas-deficient B6-lpr mice (negative and positive controls, respectively). **(D, E)** Representative FACS plots **(D)** and **(E)** summary bar graph of the frequency of $CD3^+B220^+$ double negative lymphocytes in the spleens of recipient and control mice. **(**F**)** Summary bar graphs of levels of anti-nuclear antibody (ANA) Ig (top) and anti-dsDNA Ig (bottom) as measured by ELISA. **(G, H)** Summary bar graphs demonstrating the persistence **(G)** and surface phenotype **(H)** of transferred $Thy1.1^+$ T cells modified with $Fas^{\Delta DD}$ DNR or an empty vector control. *n*=2-7 mice per cohort. ****P<0.0001, ***P<0.001, **P<0.01, *P<0.05, ns = not significant (one-way ANOVA, corrected with Tukey's multiple comparisons).

Supplemental Figure 7:

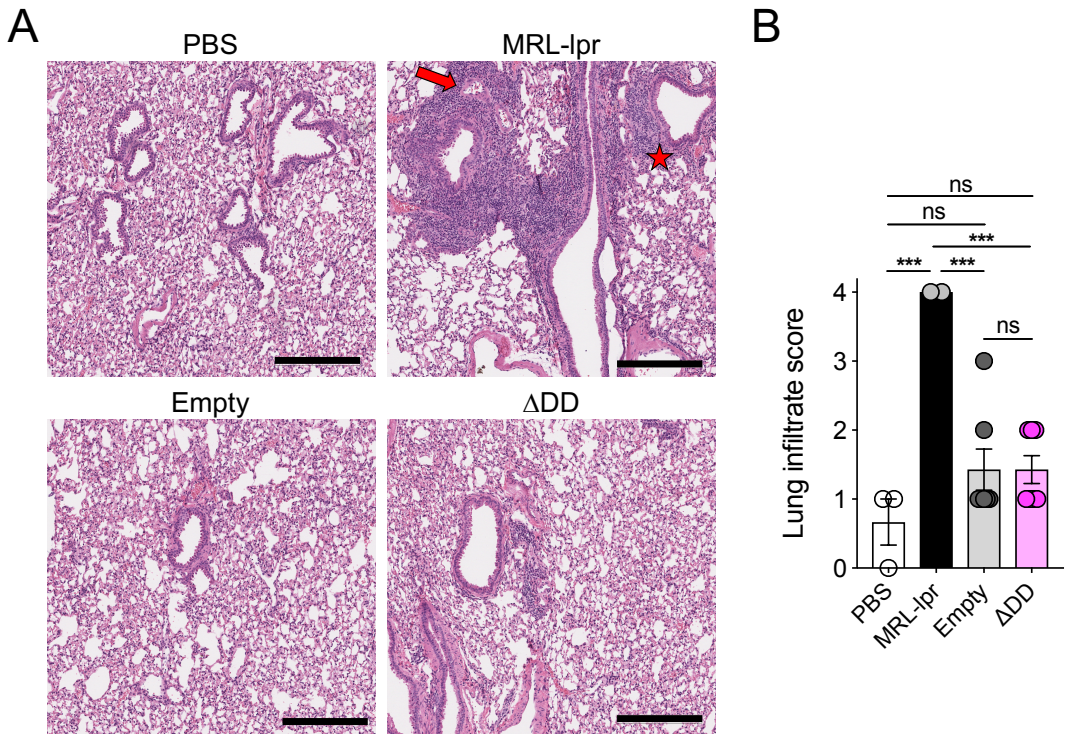

Supplemental Figure 7: Adoptively transferred T cell modified with Fas DNR do not induce an inflammatory infiltrate in the lungs of ALPS-susceptible MRL host mice. (**A**) Representative H&E stained micrographs and (**B**) summary graph demonstrating the intensity of inflammatory mononuclear cell infiltrates in the lungs of treated mice. The red arrow and red star point to areas of dense peri-vascular and peri-bronchiolar mononuclear inflammatory infiltrates, respectively. Scale bar = 300 μm. All images were scored in a blinded fashion by an interpreting pathologist. ***P<0.001, ns = not significant (one-way ANOVA, corrected with Tukey's multiple comparisons).

Supplemental Figure 8:

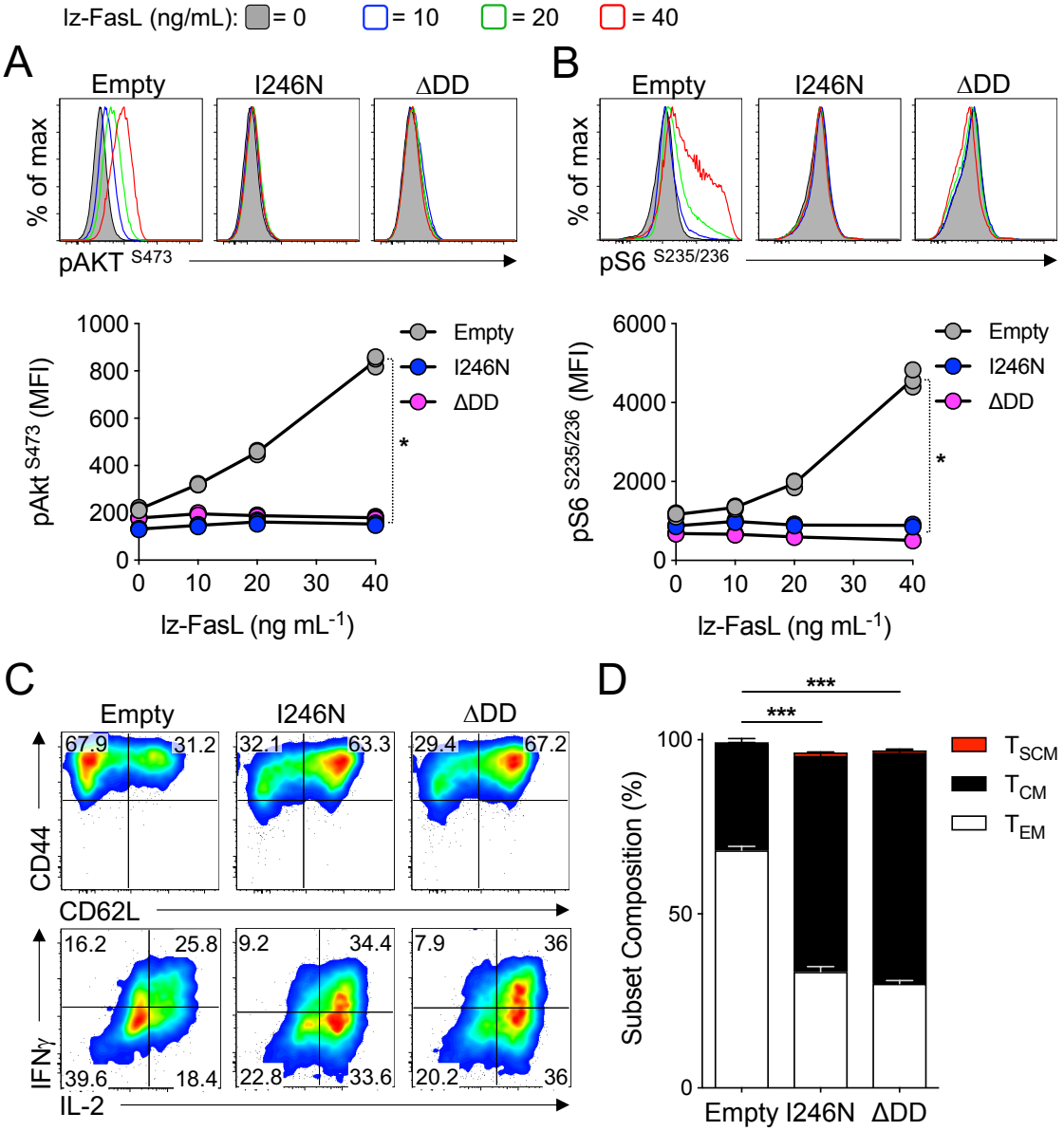

Supplemental Figure 8: Fas DNRs prevent lz-FasL-induced Akt activation and T cell differentiation. (A, B) Representative FACS histograms (top) and summary plot (bottom) of the dose-response relationship between lz-FasL exposure and (**A**) phospho- (p) Akt^{S473} and (**B**) pS6$^{S235/236}$ in CD8α^{+} T cells transduced with Fas^{I246N}, Fas$^{\Delta DD}$, or empty vector control. Results shown 6d after activation, retroviral transduction, and expansion in the continuous presence of indicated concentrations of lz-FasL. (**C**) Representative FACS plots of T cell differentiation (top) and intracellular IFNγ/IL-2 production (bottom) 11d after CD8α^{+} T cells were transduced Fas^{I246N}, Fas$^{\Delta DD}$, or empty vector control in the absence of exogenous FasL. Intracellular cytokine staining measured after ~5h incubation with PMA/ionomycin in brefeldin A and monensin. (**D**) Memory T cell subset composition of CD8α^{+} T cells 11d after activation, transduction, and expansion in culture. Graphs displayed as mean ± SEM with *n*=3 per condition and is representative of 3 (**A, B**) and 5 (**C, D**) independent experiments. **P*<0.05, (Wilcoxon rank sum test).

GTEx Tissue Type	TCGA Cancer Subtype	TCGA Abbr
Adrenal Gland	Adrenocortical Cancer	ACC
Bladder	Bladder Urothelial Carcinoma	BLCA
Whole Blood	Acute Lymphoblastic Leukemia	ALL
Brain - Amygdala Brain - Anterior Cingulate Cortex (Ba24) Brain - Caudate (Basal Ganglia) Brain - Cerebellar Hemisphere Brain - Cerebellum Brain - Cortex Brain - Frontal Cortex (Ba9) Brain - Hippocampus Brain - Hypothalamus Brain - Nucleus Accumbens (Basal Ganglia) Brain - Putamen (Basal Ganglia) Brain - Spinal Cord (Cervical C-1) Brain - Substantia Nigra	Brain Lower Grade Glioma	LGG
Brain - Amygdala Brain - Anterior Cingulate Cortex (Ba24) Brain - Caudate (Basal Ganglia) Brain - Cerebellar Hemisphere Brain - Cerebellum Brain - Cortex Brain - Frontal Cortex (Ba9) Brain - Hippocampus Brain - Hypothalamus Brain - Nucleus Accumbens (Basal Ganglia) Brain - Putamen (Basal Ganglia) Brain - Spinal Cord (Cervical C-1) Brain - Substantia Nigra	Glioblastoma Multiforme	GBM
Breast - Mammary Tissue	Breast Invasive Carcinoma	BRCA
Cervix - Ectocervix Cervix - Endocervix	Cervical & Endocervical Cancer	CESC
Kidney - Cortex	Kidney Clear Cell Carcinoma	KIRC
Kidney - Cortex	Kidney Renal Papillary Cell Carcinoma	KIRP
Colon - Sigmoid Colon - Transverse	Colon Adenocarcinoma	COAD
Colon - Sigmoid	Rectum Adenocarcinoma	READ
Esophagus - Gastroesophageal Junction Esophagus - Mucosa	Esophageal Carcinoma	ESCA
Liver	Liver Hepatocellular Carcinoma	LIHC
Lung	Lung Adenocarcinoma	LUAD
Lung	Lung Squamous Cell Carcinoma	LUSC
Spleen	Diffuse Large B-Cell Lymphoma	DLBC
Adipose - Subcutaneous Artery - Tibial Nerve - Tibial Muscle - Skeletal	Sarcoma	SARC
Fallopian Tube Ovary	Ovarian Serous Cystadenocarcinoma	OV
Prostate	Prostate Adenocarcinoma	PRAD
Pancreas	Pancreatic Adenocarcinoma	PAAD
Skin - Not Sun Exposed (Suprapubic) Skin - Sun Exposed (Lower Leg)	Skin Cutaneous Melanoma	SKCM
Stomach	Stomach Adenocarcinoma	STAD
Testis	Testicular Germ Cell Tumor	TGCT
Thyroid	Thyroid Carcinoma	THCA
Uterus	Uterine Carcinosarcoma	UCS
Uterus	Uterine Corpus Endometrioid Carcinoma	UCEC

Supplemental Table 1: Summary of TCGA cancer subtypes and matched tissues of origin from the GTEx database. A list of the normal tissues of origin and corresponding cancer subtypes (*n*=26) were obtained from the GTEx and TCGA datasets, respectively.

Gene	*r*	Gene	*r*	Gene	*r*	Gene	*r*	Gene	*r*
SLA2	0.8580	*CCL5*	0.6757	*NCKAP1L*	0.6194	*ZAP70*	0.5731	*PTPRCAP*	0.5407
CD8A	0.8539	*ARHGAP9*	0.6747	*LILRB1*	0.6157	*NCR1*	0.5723	*CD96*	0.5387
CCR5	0.8510	*KLRD1*	0.6742	*SIT1*	0.6144	*MS4A6A*	0.5721	*STAT1*	0.5375
CD2	0.8440	*SLFN12L*	0.6739	*GNGT2*	0.6142	*LCK*	0.5720	*FCER1G*	0.5374
NKG7	0.8394	*ARHGAP30*	0.6597	*C1QA*	0.6137	*ARHGAP15*	0.5680	*CST7*	0.5370
GZMA	0.8383	*ZNF683*	0.6593	*TNFAIP8L2*	0.6107	*CD86*	0.5667	*IGFLR1*	0.5366
KLRK1	0.8337	*IL10RA*	0.6583	*APOL3*	0.6092	*LAIR1*	0.5656	*TRAF3IP3*	0.5364
CRTAM	0.8205	*IL18BP*	0.6576	*FCGR1B*	0.6073	*GBP1*	0.5605	*HLA-DMA*	0.5362
CXCR6	0.8097	*TRAT1*	0.6512	*TLR8*	0.6069	*CD200R1*	0.5605	*CYBB*	0.5360
SIRPG	0.8039	*ABCD2*	0.6506	*DOCK2*	0.6052	*CD4*	0.5594	*LAT*	0.5342
IFNG	0.8036	*GPR65*	0.6502	*IKZF1*	0.6031	*GBP2*	0.5590	*TNFRSF1B*	0.5342
UBASH3A	0.8005	*SASH3*	0.6493	*LTA*	0.6025	*ABI3*	0.5580	*ITGB2*	0.5334
EOMES	0.8000	*CD6*	0.6478	*ARHGAP25*	0.6021	*HLA-E*	0.5577	*CD3G*	0.5329
PRF1	0.7911	*SLAMF7*	0.6440	*HLA-DPB1*	0.6015	*PLEK*	0.5570	*TBC1D10C*	0.5304
CD247	0.7882	*CYTH4*	0.6436	*TTC24*	0.6014	*LAPTM5*	0.5557	*TRIM22*	0.5290
PYHIN1	0.7822	*FAM78A*	0.6416	*C1QC*	0.5971	*SAMHD1*	0.5553	*JAK3*	0.5289
CD3E	0.7818	*PTPRC*	0.6414	*GIMAP2*	0.5962	*ZNF80*	0.5547	*CIITA*	0.5288
CD3D	0.7780	*XCL2*	0.6397	*BTN3A2*	0.5936	*CORO1A*	0.5542	*B2M*	0.5280
LAG3	0.7708	*RASAL3*	0.6395	*WIPF1*	0.5896	*IL16*	0.5531	*GAB3*	0.5265
GZMH	0.7693	*CD74*	0.6386	*TIFAB*	0.5893	*CLEC2D*	0.5506	*SIGLEC10*	0.5264
CCL4	0.7582	*IRF1*	0.6385	*GIMAP4*	0.5892	*C5orf56*	0.5503	*VAV1*	0.5263
CXCR3	0.7568	*SEPT1*	0.6366	*TNFRSF9*	0.5889	*GBP5*	0.5494	*TAP1*	0.5254
GPR174	0.7559	*ITK*	0.6359	*APOBEC3H*	0.5887	*LILRB2*	0.5467	*CXorf21*	0.5239
GZMK	0.7358	*CD53*	0.6358	*FCGR3A*	0.5885	*CARD16*	0.5464	*CD160*	0.5232
TIGIT	0.7333	*BIN2*	0.6340	*IL18RAP*	0.5873	*HLA-DQA1*	0.5463	*NCF1*	0.5203
ITGAL	0.7237	*GRAP2*	0.6332	*CCR2*	0.5869	*P2RY13*	0.5462	*GIMAP5*	0.5200
IL12RB1	0.7188	*AC008964.1*	0.6305	*CD48*	0.5851	*HLA-DOA*	0.5458	*PTPN7*	0.5199
LCP2	0.7133	*MYO1F*	0.6296	*CD72*	0.5851	*FMNL1*	0.5452	*FERMT3*	0.5190
PDCD1	0.7126	*IL21R*	0.6285	*LAP3*	0.5846	*SCIMP*	0.5446	*LST1*	0.5189
SAMD3	0.7113	*BTN3A3*	0.6265	*APOBEC3D*	0.5836	*C1orf162*	0.5446	*ITGAE*	0.5188
FAM26F	0.7050	*ICOS*	0.6242	*SELPLG*	0.5808	*IGSF6*	0.5438	*IL2RB*	0.5180
SNX20	0.6990	*PVRIG*	0.6240	*DOK2*	0.5803	*PSMB9*	0.5435	*SAMSN1*	0.5160
CTSW	0.6979	*SLAMF8*	0.6235	*AD000671.6*	0.5802	*EVI2A*	0.5434	*BTN2A2*	0.5152
FCRL6	0.6945	*C1QB*	0.6235	*AIF1*	0.5797	*HLA-DRB1*	0.5421	*GMFG*	0.5139
PSTPIP1	0.6945	*HLA-DPA1*	0.6229	*SLA*	0.5780	*FYB*	0.5420	*GIMAP7*	0.5119
HCST	0.6833	*HLA-DRA*	0.6224	*APOBEC3G*	0.5778	*PARVG*	0.5419	*APOL6*	0.5112
SLAMF6	0.6826	*TBX21*	0.6219	*GBP4*	0.5776	*P2RY10*	0.5414	*NLRC5*	0.5099
SPN	0.6803	*BTN3A1*	0.6217	*ACAP1*	0.5762	*LILRB4*	0.5412	*LY9*	0.5092
CXCL9	0.6795	*FCGR1A*	0.6216	*SP140*	0.5752	*WAS*	0.5410	*GPR31*	0.5087
KLRC4-KLRK1	0.6773	*KLRC4*	0.6200	*EVI2B*	0.5744	*C15orf53*	0.5408	*AKNA*	0.5087

Supplemental Table 2: A pan-cancer analysis of the top 200 genes positively correlated with *FASLG* across the TCGA dataset. Gene names and Pearson's correlation coefficient (*r*) to *FASLG* are listed.